HHS Public Access

Author manuscript

J Bone Miner Res. Author manuscript; available in PMC 2021 February 01.

Published in final edited form as:

J Bone Miner Res. 2020 February ; 35(2): 382–395. doi:10.1002/jbmr.3882.

Alveolar bone protection by targeting the SH3BP2-SYK axis in osteoclasts

Mizuho Kittaka[1,2], **Tetsuya Yoshimoto**[1,2], **Collin Schlosser**[3], **Robert Rottapel**[4], **Mikihito Kajiya**[5], **Hidemi Kurihara**[5], **Ernst J Reichenberger**[6], **Yasuyoshi Ueki**[1,2]

[1]Department of Biomedical Sciences and Comprehensive Care, Indiana University School of Dentistry, Indianapolis, IN, 46202 USA

[2]Indiana Center for Musculoskeletal Health, Indiana University School of Medicine, Indianapolis, IN, 46202 USA

[3]Department of Orthodontics and Dentofacial Orthopedics, University of Missouri-Kansas City, School of Dentistry, Kansas City, MO, 64108 USA

[4]Department of Medicine, Immunology and Medical Biophysics, University of Toronto, Toronto, ON M5S 1L7, Canada

[5]Department of Periodontal Medicine, Applied Life Sciences, Institute of Biomedical & Health Sciences, Graduate School of Biomedical & Health Sciences, Hiroshima University, Hiroshima, 734-8553 Japan

[6]Department of Reconstructive Sciences, School of Dental Medicine, University of Connecticut Health, Farmington, CT 06030, USA

Abstract

Periodontitis is a bacterially induced chronic inflammatory condition of the oral cavity where tooth-supporting tissues including alveolar bone are destructed. Previously, we have shown that the adaptor protein SH3-domain binding protein 2 (SH3BP2) plays a critical role in inflammatory response and osteoclastogenesis of myeloid lineage cells through spleen tyrosine kinase (SYK). In this study, we show that SH3BP2 is a novel regulator for alveolar bone resorption in periodontitis. MicroCT analysis of SH3BP2-deficient (*Sh3bp2*$^{-/-}$) mice challenged with ligature-induced periodontitis revealed that *Sh3bp2*$^{-/-}$ mice develop decreased alveolar bone loss (male: 14.9 ± 10.2%, female: 19.0 ± 6.0%) compared to wild-type control mice (male: 25.3 ± 5.8%, female: 30.8 ± 5.8%). Lack of SH3BP2 did not change the inflammatory cytokine expression and osteoclast induction. Conditional knockout of SH3BP2 and SYK in myeloid lineage cells with

Corresponding author: Yasuyoshi Ueki, M.D., Ph.D., Department of Biomedical Sciences and Comprehensive Care, Indiana University School of Dentistry, Indiana Center for Musculoskeletal Health, Indiana University School of Medicine, 635 Barnhill Dr., Van Nuys Medical Science Bldg. Room#514, Indianapolis, Indiana 46202, USA TEL: +1-317-278-6580, Fax: +1-317-278-6500, uekiy@iu.edu.

Authors' roles: YU conceived the project idea. MK and YU initiated the project. MK, TY, MK, HK, and YU designed the experiments. MK, TY, CS performed experiments. RR provided the global SH3BP2 knockout mice for this project and contributed to data interpretation. EJR contributed to study design and data interpretation. All authors contributed to the data analysis. MK and YU wrote the manuscript, and all authors approved the manuscript. YU and MK are responsible for data integrity and analysis.

Disclosure

The authors have declared that no conflict of interest exists.

LysM-Cre mice recapitulated the reduced bone loss without affecting both inflammatory cytokine expression and osteoclast induction, suggesting that the SH3BP2-SYK axis plays a key role in regulating alveolar bone loss by mechanisms that regulate the bone-resorbing function of osteoclasts rather than differentiation. Administration of a new SYK inhibitor GS-9973 before or after periodontitis induction reduced bone resorption without affecting inflammatory reaction in gingival tissues. *In vitro*, GS-9973 treatment of bone marrow-derived M-CSF-dependent macrophages suppressed tartrate-resistant acid phosphatase (TRAP)-positive osteoclast formation with decreased mineral resorption capacity even when GS-9973 was added after RANKL stimulation. Thus, the data suggest that SH3BP2-SYK is a novel signaling axis for regulating alveolar bone loss in periodontitis and that SYK can be a potential therapeutic target to suppress alveolar bone resorption in periodontal diseases.

Keywords

Periodontitis; SH3BP2; SYK; Bone loss; Osteoclasts

Introduction

Periodontitis is a chronic oral inflammatory disorder with periodontal tissue destruction caused by pathogenic bacteria. Damage of gingival tissue in periodontitis provides oral bacteria with an infection route toward multiple organs, resulting in harmful events in health such as atherosclerotic disease, adverse pregnancy, rheumatoid arthritis (RA), and inflammatory bowel disease.[1,2] According to a recent study, periodontitis is a highly prevalent disease that affects 47% of adults in the USA[3] and is the most common cause of alveolar bone loss responsible for tooth loss[4]. Periodontitis is the result of a cascade of inflammatory immune response initiated by bacterial invasion. Innate immune cells in periodontal tissues such as neutrophils and macrophages recognize pathogenic components of several bacteria species in dental plaque via pattern recognition receptors (PRRs) such as toll-like receptors (TLRs) and nucleotide oligomerization domain (NOD)-like receptors (NLRs).[5] Innate immune cells stimulated by pathogens produce abundant pro-inflammatory cytokines such as tumor necrosis factor (TNF)-α, interleukin (IL)-1β, IL-6, IL-8, and interferon (IFN)-γ to accelerate immune responses that induce subsequent activation of the acquired immune system.[4] T helper 17 (T_H17) cells are the key drivers for pathogenic mucosal inflammation in periodontitis[6–8] and expansion of T_H17 cells is dependent on the local dysbiotic microbiome.[8] T_H17 cells also function as an osteoclastogenic helper T cell subset in inflammatory bone destruction.[9,10]

Osteoclasts are exclusively responsible for alveolar bone resorption in the sequence of events during periodontitis[4,5,11–13] and receptor activator of nuclear factor-kappaB ligand (RANKL), which is a member of the TNF cytokine family, is a pivotal cytokine for osteoclastogenesis.[14–16] Recently, it has been shown that osteoblasts and periodontal ligament cells as well as osteocytes are primary sources of RANKL for osteoclastogenesis in mouse experimental periodontitis models.[17,18] Notably, IL-17 produced by T_H17 cells induces RANKL expression by osteoblastic and periodontal ligament cells in a ligature-

induced periodontitis model[17] and stimulates RANKL production by osteocytes in a bone loss model using continuous parathyroid hormone (PTH) treatment.[19]

The SH3-domain binding protein 2 (SH3BP2) is an adaptor protein dominantly expressed in hematopoietic lineage cells such as neutrophils, T cells, B cells, and macrophages. SH3BP2 interacts with several proteins including spleen tyrosine kinase (SYK), 14-3-3, VAV, LYN, SHP-1, PLCγ1/2, indicating that SH3BP2 is involved in a variety of cellular functions.[20–31] Gain-of-function mutations in SH3BP2 are responsible for a human craniofacial disorder, cherubism (OMIM#118400).[32] Analysis of a knock-in mouse model for cherubism revealed that a cherubism mutation increases osteoclastogenesis induced by RANKL and TNF-α and enhances macrophage responsiveness to pathogen-associated molecular patterns (PAMPs) via TLRs.[33–35] SYK is critically required for the increased activation of osteoclasts and macrophages carrying cherubism mutations.[33–35] The SH3BP2 gain-of-function mutation also alters the manifestation of autoimmune diseases in mice.[36,37] In contrast, loss-of-function of SH3BP2 suppresses osteoclast function[38,39] and reduces inflammation and joint destruction in mouse models for RA.[39] Thus, investigations from our group have established that SH3BP2 is a regulator of inflammation and osteoclastogenesis and demonstrated that the SH3BP2-SYK axis, as a key signaling pathway in the osteoimmune system, is involved in the pathological mechanisms of common inflammatory arthritis beyond its role in a rare craniofacial disorder.

Since aberrant regulation of inflammatory response and osteoclastic bone resorption are the hallmarks of periodontitis, we hypothesized that SH3BP2 also mediates alveolar bone resorption in periodontitis. Here, we show that loss-of-function of SH3BP2 reduces susceptibility to alveolar bone loss in a ligature-induced periodontitis model. Deletion of SH3BP2 in myeloid lineage cells is sufficient for the reduced susceptibility without altering the induction of tartrate-resistant acid phosphatase (TRAP)-positive osteoclasts, the expression profile of inflammatory cytokines in gingiva, or the composition of oral microbiota. Lack of SYK, a key kinase interacting with SH3BP2, in myeloid cells also provides comparable protection against alveolar bone loss. Pharmacological inhibition of SYK by GS-9973 not only prevents alveolar bone loss but also ameliorates progressive alveolar bone resorption in a ligature-induced periodontitis model. Indeed, GS-9973 treatment suppresses TRAP-positive osteoclast formation with a reduced capacity for mineral resorption *in vitro*. Our study demonstrates that the SH3BP2-SYK axis regulates alveolar bone resorption in periodontitis and suggests that SYK can be a target for preventing or treating alveolar bone resorption associated with periodontal diseases.

Materials and Methods

Mice

All animal experiments in this study were performed according to protocols approved by the IACUCs of the University of Missouri-Kansas City and Indiana University. *Sh3bp2*$^{-/-}$ mice have been created previously.[40] *LysM-Cre* mice (#004781) and *Syk*$^{fl/fl}$ mice (#017309) were obtained from the Jackson Laboratory (Bar Harbor, Maine, USA). All mice were bred in a C57BL/6J background and housed under specific-pathogen-free conditions.

Generation of Sh3bp2 floxed mice

Sh3bp2-floxed (*Sh3bp2*$^{fl/fl}$) mice were generated by inGenious Targeting Laboratory (Ronkonkoma, NY, USA). The targeting construct harboring *Sh3bp2* exon 3 flanked by loxP sites and a neomycin-resistance cassette flanked by Frt sites was electroporated to hybrid (C57BL/6 x 129/SvEv) ES cells (Supplemental Fig. S1). Electroporated ES cells were then cultured in medium containing G418 for positive selection. Targeted ES cell clones were identified by PCR and confirmed by Southern blot, and one of the ES cell clones was used for generating chimera mice. Chimera mice were bred with FLP transgenic mice for *in vivo* excision of the neomycin cassette. Mice carrying a *Sh3bp2*-floxed allele in germline were backcrossed to C57BL/6J mice for at least 7 generations (N=7) and used for experiments.

A ligature-induced periodontitis model

5-0 silk suture (Ethicon, Somerville, NJ, USA) was tied around the maxillary left second molar of 10-week-old mice under anesthesia with ketamine (80 mg/kg) and xylazine (1 mg/kg). The right second molar was untreated and served as the control for alveolar bone volume analysis. After 5 days of ligature placement, mice were euthanized and the maxilla was dissected out for analysis. Mice that were treated with antibiotics received an antibiotic cocktail in drinking water (ampicillin 1 g/L, vancomycin 0.5 g/L, kanamycin 1 g/L, metronidazole 1 g/L) *ad libitum* from 5 days before ligature placement until the day of analysis.

Ex-vivo microCT (μCT) analysis

Maxillae were subjected to alveolar bone analysis with μCT. Tissues were fixed with 4% paraformaldehyde (PFA) for 24 hours and soaked in 70% ethanol for a scan with the Skyscan1174 (Bruker, Kontich, Belgium) under the following conditions: 80 kV X-ray energy, 6.67 μm pixel size, and 0.4 degree rotation step with 3000 ms of exposure time. Scanned data were reconstructed with NRecon software (Bruker) with a dynamic image range from 0 to 0.22. Alignment of three-dimensional (3D) images was performed using the DataViewer (Bruker) with the occlusal plane oriented parallel to the transverse plane. The region of interest (ROI) for bone volume measurement was alveolar bone between two buccal roots underneath the second molar that is composed of 21 2D slices (approximately 140 μm thickness). Segmentation of the ROI and following bone volume measurement were performed by CT-Analyser (Bruker) with a threshold value of 44. Susceptibility for alveolar bone loss (% reduction rate) was calculated with the following formula: {(bone volume of unligated side − bone volume of ligated side)/bone volume of unligated side} x 100. 3D images were created by CTVox software (Bruker) based on the volume rendering method.

16S rDNA amplicon sequencing

Ligatures were recovered 5 days after ligature placement. Each suture was vortexed in 500 μL of sterile PBS for 3 minutes. Bacterial DNA was isolated using Meta-G-Nome DNA Isolation Kit (Epicentre, Madison, WI, USA). Isolated DNAs were used for 16S rDNA amplicon analysis at BGI America (Cambridge, MA, USA). The V4 region of 16S rDNA was amplified by PCR and PCR products were used for library construction followed by

sequencing and data analysis. Ribosomal Database Project Classifier v. 2.2 was used for taxonomic classification.[41]

RNA isolation from gingiva and jawbone

Maxillary gingival tissues (1 x 3 mm) at the palatal side and maxillary alveolar bone tissues including three molars from mice with ligatures on both sides were used for RNA extraction. Dissected gingival tissue was homogenized by a tissue grinder (Thermo Fisher Scientific, Waltham, MA, USA). Jawbones were snap-frozen in liquid nitrogen after removing soft tissues, then crushed into powder using a tissue pulverizer (Cellcrusher Limited, Portland, OR, USA). RNA was extracted by RiboZol RNA extraction reagent (Amresco, Solon, OH, USA). RNA samples from mice without ligatures were used for controls.

Reverse transcription-qPCR (RT-qPCR) analysis

Five hundred ng of total RNA was transcribed to cDNA using a High Capacity cDNA Reverse Transcription Kit (Applied Biosystems, Foster City, CA, USA). qPCR reactions were performed with StepOnePlus Real-Time PCR System (Applied Biosystems) using Maxima SYBR Green qPCR Master Mix (Thermo Fisher Scientific). qPCR primers used in this study are listed in Supplemental Table 1. Relative gene expression levels were calculated using the relative-standard curb method. Each gene expression level was normalized by the expression level for *Hprt*.

Histology

Maxillae were fixed with 4% PFA for 24 hours, decalcified with EDTA (0.5M, pH 7.2) and embedded in paraffin. Six-μm sections cut in the sagittal plane were subjected to H&E and TRAP staining.

Histomorphometry for osteoclasts

After TRAP staining, the number of osteoclasts (N.Oc), osteoclast surface (Oc.S), bone surface (BS), and the number of osteoclasts with ruffled border at alveolar bone between 2 buccal roots of the maxillary second molar were measured using Bioquant Osteo software (Bioquant Image Analysis Corporation, Nashville, TN, USA). Either bone samples from unligated mice or from the unligated right side were used as controls. Two tissue sections separated by 20-50 μm were measured for each mouse and averaged. Measurements were performed by personnel blinded to genotypes and inhibitor administration.

SYK inhibitor treatment

Mice were administered with entospletinib daily (GS-9973, 100 mg/kg/day, intraperitoneally, MedChemExpress, Monmouth Junction, NJ, USA) starting from one day before or 2 days after ligature placement until the day of analysis.

Osteoclast differentiation assay

Bone marrow cells were collected from tibia, femur, and ilium of 6- to 12-week-old mice. After removal of red blood cells with RBC lysis buffer, bone marrow cells were incubated with alpha-MEM supplemented with 10% FBS and penicillin/streptomycin for 3 hours on

petri dishes to allow stromal cells to adhere to the dishes. Non-adherent cells were collected and seeded on 48-well plates at a density of 5.0 x 10^4 cells/well and incubated in the presence of M-CSF (25 ng/mL, PeproTech, Rocky Hill, NJ, USA) for 2 days to obtain bone marrow-derived M-CSF-dependent macrophages (BMMs, set as day 0 in Fig. 6C, 6D, 6E). BMMs were further stimulated with M-CSF (25 ng/mL) and RANKL (50 ng/mL, PeproTech), RANKL/TNF-α (100 ng/ml, PeproTech), or RANKL/IL-1β (10 ng/mL, PeproTech) for up to 4 days with or without GS-9973. To examine the effect of GS-9973 at the middle stage of osteoclast differentiation, GS-9973 treatment was started 1 day or 2 days after RANKL stimulation. Culture media were changed every other day. TRAP-positive cells were visualized with a TRAP staining kit (Sigma-Aldrich, St. Louis, MO, USA), and TRAP-positive cells with more than 3 nuclei were counted as osteoclasts (TRAP+ MNCs).

Osteoclast resorption assay

Non-adherent cells from bone marrow were seeded on 96-well Osteo assay plates (Corning, Corning, NY, USA) at a density of 2.0 x 10^4 cells/well and incubated in the presence of M-CSF (25 ng/mL) for 2 days. BMMs were further stimulated with M-CSF (25 ng/mL) and RANKL (50 ng/mL) with or without GS-9973 (0.001 to 1 μM) for 10 days. After removing cells from the plate surface with 10% bleach solution for 5 min at room temperature, resorption areas were visualized by von Kossa staining.

Phalloidin staining

Non-adherent cells from bone marrow were seeded on 8-well chamber slides (Corning) at a density of 3.7 x 10^4 cells/well and cultured with M-CSF for 2 days to obtain BMMs. BMMs were stimulated with M-CSF and RANKL for 3 days to induce osteoclast differentiation with or without GS-9973 (1.0 μM). Cells were fixed with 4% PFA, permeabilized with 0.25% Triton X-100 in PBS, then blocked with 1% BSA in PBS. Cells were stained with Alexa Fluor-488 conjugated phalloidin and DAPI (Santa Cruz Biotechnology, Dallas, USA). Fluorescent images were acquired with a Keyence BZ-X800 microscope (Keyence, Osaka, Japan).

Western blotting

3.0 x 10^6 non-adherent cells from bone marrow were seeded on 100 mm cell culture dishes and pre-cultured with M-CSF (25 ng/mL) for 2 days. RANKL (50 ng/mL) was added to the BMM culture for up to 4 days with or without GS-9973. At each time point, BMMs were lysed with cell lysis buffer (1% Triton X-100, 25 mM Tris-HCl (pH 7.4), 150 mM NaCl, 5 mM EDTA, 10% glycerol, 2.5 mM sodium pyrophosphate, 0.7 mM β-glycerophosphate) with protease and phosphatase inhibitor cocktails (Sigma-Aldrich, St. Louis, MO). Five micrograms of protein samples were resolved by SDS-PAGE under reducing conditions and transferred to nitrocellulose membranes. After blocking with 5% skim milk in TBS supplemented with 1% Tween-20 (TBST), membranes were incubated with anti-MMP9 (ab38898, Abcam), anti-Cathepsin K (ab19027, Abcam), anti-NFATc1 (7A6, Santa Cruz), anti-SRC (32G6, Cell Signaling Technology, Danvers, MA), anti-ACTIN (A2066, Sigma-Aldrich) in 5% BSA/TBST overnight at 4°C followed by incubation with HRP-conjugated secondary antibodies (Cell Signaling Technology). Anti-SYK (D3Z1E, Cell Signaling Technology) and anti-SH3BP2 (1E9, Abnova, Taipei City, Taiwan) antibodies were used for

BMMs stimulated with M-CSF for 4 days without RANKL stimulation. Bands were detected using SuperSignal West Dura or Femto chemiluminescent substrates (Thermo Fisher Scientific) and visualized by a Celvin S320 Imager (biostep, Burkhardtsdorf, Germany).

Statistics

Statistical analysis was performed by the two-tailed unpaired Student's *t*-test to compare two groups or by one-way ANOVA with Tukey-Kramer post hoc test to compare three or more groups. GraphPad Prism 8 (GraphPad Software, La Jolla, CA, USA) and SPSS Statistics 20 (IBM, Armonk, NY, USA) were used for all statistical analyses. Any p values less than 0.05 were considered to be significant.

Results

Loss-of-function of SH3BP2 reduces alveolar bone loss in a ligature-induced periodontitis model

To determine the role of SH3BP2 in the pathoetiology of periodontitis, a mouse ligature-induced periodontitis model was applied to the SH3BP2 knockout mice (*Sh3bp2*$^{-/-}$), where an increased oral bacterial load due to accumulation of commensal bacteria within the silk ligature is responsible for periodontal inflammation and subsequent alveolar bone resorption.[42] This ligature model has been widely used to study the molecular mechanisms of periodontitis.[6,17,43] To confirm that ligature-induced periodontitis is dependent on bacterial accumulation surrounding a ligated tooth, we treated a group of 10-week-old wild-type mice with an antibiotic cocktail (ampicillin, vancomycin, kanamycin, metronidazole) in drinking water from 5 days before ligature placement. MicroCT (μCT) analysis showed that antibiotic treatment suppresses alveolar bone loss (Supplemental Fig. S2). This result confirmed that the increased bacterial load around the gingiva is a primary trigger for alveolar bone resorption in this model.

Next, we induced periodontitis in *Sh3bp2*$^{+/+}$ and *Sh3bp2*$^{-/-}$ mice and compared the susceptibility to bone loss. Ligature placement caused alveolar bone loss in *Sh3bp2*$^{+/+}$ and *Sh3bp2*$^{-/-}$ mice (Fig. 1A). μCT analysis showed that alveolar bone volume of the unligated right side is not significantly different between *Sh3bp2*$^{+/+}$ and *Sh3bp2*$^{-/-}$ mice. However, significantly more alveolar bone was maintained on the ligated left side of *Sh3bp2*$^{-/-}$ mice compare to *Sh3bp2*$^{+/+}$ mice (Fig. 1B, top). Calculation of susceptibility to bone loss (% bone loss) against the unligated side revealed that male *Sh3bp2*$^{-/-}$ mice had 41.1% less bone loss and female *Sh3bp2*$^{-/-}$ mice had 38.3% less bone loss than *Sh3bp2*$^{+/+}$ mice (Fig. 1B, bottom). Because loss-of-function of SH3BP2 causes defects in immune cell response *in vitro* and *in vivo,*[31,39,40,44] we hypothesized that knocking out *Sh3bp2* may reduce inflammation in the gingiva and that the lower susceptibility to alveolar bone loss in *Sh3bp2*$^{-/-}$ mice may be attributed to reduced inflammation. However, H&E staining showed comparable amounts of inflammatory cell infiltration underneath the suture in *Sh3bp2*$^{+/+}$ and *Sh3bp2*$^{-/-}$ mice (Fig. 1C). Supporting this result, qPCR analysis of gingival tissue showed comparable expression levels of *Ly6g*, a marker gene for neutrophils, and *Cxcr2,* a receptor for chemokines expressed in granulocytes and neutrophils, between ligated

Sh3bp2$^{+/+}$ and *Sh3bp2*$^{-/-}$ mice (Fig. 1D). Expression levels for genes associated with periodontitis progression and osteoclastic bone resorption such as *Il1β*, *Il6*, *Tnf*, and *Il17a* in gingiva were not significantly different between the two ligated groups (Fig. 1E).

Next, we asked whether loss-of-function of SH3BP2 causes a dysbiotic change in the oral microbiome that may be associated with a reduction in alveolar bone loss in *Sh3bp2*$^{-/-}$ mice. We examined the taxonomic composition of bacteria that accumulated in the silk suture. Taxonomic analysis on an order level showed that the bacteria flora is mostly composed of *Pasteurellales, Lactobacillales, Bacteroidales, Bifidobacteriales, Erysipelotrichales*, and *Enterobacteriales* and the composition of each order of bacteria is comparable between *Sh3bp2*$^{+/+}$ and *Sh3bp2*$^{-/-}$ mice (Supplemental Fig. S3). This result suggests that loss-of-function of SH3BP2 does not alter the oral bacterial flora and that a dysbiotic change is not responsible for the reduced alveolar bone loss in *Sh3bp2*$^{-/-}$ mice. Taken together, these data show that loss-of-function of SH3BP2 decreases alveolar bone loss without affecting gingival inflammation or the composition of oral microbiota in a ligature-induced periodontitis model.

Loss-of-function of SH3BP2 does not alter osteoclast induction in ligature-induced periodontitis

Because osteoclasts are the predominant cells responsible for inflammatory bone resorption, we investigated whether loss-of-function of SH3BP2 affects osteoclast induction in ligature-induced periodontitis. TRAP staining showed that ligature placement induces osteoclasts on the alveolar bone surface in both *Sh3bp2*$^{+/+}$ and *Sh3bp2*$^{-/-}$ mice (Fig. 2A). Those osteoclasts did form ruffled borders (Fig. 2B). However, histomorphometric analysis for osteoclasts revealed that there is no significant difference in the number of osteoclasts/bone surface (N.Oc/BS), osteoclast surface/bone surface (Oc.S/BS), or percentage of osteoclasts with ruffled borders between the *Sh3bp2*$^{+/+}$ and *Sh3bp2*$^{-/-}$ groups (Fig. 2C). Since osteoblasts and periodontal ligament cells as well as osteocytes are primary sources for RANKL for osteoclastogenesis in mouse experimental periodontitis models,[17,18] we investigated *Rankl* levels in gingiva and jawbone. Baseline levels of *Rankl* in jawbone of unligated mice were higher in *Sh3bp2*$^{-/-}$ mice than in *Sh3bp2*$^{+/+}$ mice. *Rankl* levels in ligated mice were similar in male *Sh3bp2*$^{-/-}$ and *Sh3bp2*$^{+/+}$ mice, but significantly higher in female *Sh3bp2*$^{-/-}$ mice compared to *Sh3bp2*$^{+/+}$ mice. Gingival tissue was not a major RANKL source in ligature-induced periodontitis (Fig.2D). Osteoprotegerin (*Opg)* levels and *Rankl/Opg* ratio were comparable between *Sh3bp2*$^{+/+}$ and *Sh3bp2*$^{-/-}$ mice in both unligated and ligated conditions (Fig.2D).

qPCR analysis for marker genes of osteoclast differentiation and function showed that expression levels of *Acp5*, *Oscar*, and *Ocstamp* do not correlate with decreased jawbone loss in *Sh3bp2*$^{-/-}$ mice, although induction of *Ctsk*, which codes for Cathepsin K that is secreted by mature osteoclasts to degrade type I collagen, were significantly decreased in alveolar bone from ligated *Sh3bp2*$^{-/-}$ mice compared to ligated *Sh3bp2*$^{+/+}$ mice (Fig. 2E). These results suggest that reduced bone loss in *Sh3bp2*$^{-/-}$ mice is attributed to impaired function of *Sh3bp2*$^{-/-}$ osteoclasts rather than to impaired differentiation of *Sh3bp2*$^{-/-}$ osteoclasts. Previous reports that SH3BP2 is required for osteoclast function but not differentiation

under physiological conditions and that *Sh3bp2*$^{-/-}$ osteoclasts are defective in bone resorption capacity in inflammatory conditions *in vitro* support this interpretation.[38,39]

SH3BP2 in myeloid cells regulates susceptibility to alveolar bone loss in ligature-induced periodontitis

To determine whether loss-of-function of SH3BP2 in osteoclast lineage cells plays a protective role against bone loss in ligature-induced periodontitis, we created *Sh3bp2* conditional knockout mice (*Sh3bp2*$^{fl/fl}$) on *LysM-Cre* knock-in background, where *Sh3bp2* is knocked out in *LysM*-expressing myeloid lineage cells such as macrophages, osteoclasts, and neutrophils. A validation experiment for *Sh3bp2* gene deletion in bone marrow-derived M-CSF-dependent macrophages (BMMs), which are progenitors for osteoclasts, showed that homozygous expression of *LysM-Cre* (*LysM*$^{cre/cre}$) is necessary for sufficient *Sh3bp2* deletion (Supplemental Fig. S4). Therefore, we considered *LysM*$^{cre/cre}$ *Sh3bp2*$^{fl/fl}$ mice as conditional knockouts for *Sh3bp2* and used *LysM*$^{cre/cre}$ *Sh3bp2*$^{+/+}$ and/or *LysM*$^{+/+}$ *Sh3bp2*$^{fl/fl}$ mice as controls.

Lack of SH3BP2 in myeloid cells recapitulated the decreased susceptibility to alveolar bone loss of *Sh3bp2*$^{-/-}$ mice with periodontitis (Fig. 3A, 3B). Osteoclast induction in *LysM*$^{cre/cre}$ *Sh3bp2*$^{fl/fl}$ mice was comparable to control mice (Fig. 3C), which was confirmed by histomorphometric analysis of osteoclast parameters (Fig. 3D). Also lack of SH3BP2 in myeloid cells did not affect expression levels of osteoclast-related genes in jawbone or inflammatory genes in gingival tissue (Supplemental Fig. S5). Considering the fact that BMMs are precursors for osteoclasts and the inflammatory status in gingiva is not altered in *LysM*$^{cre/cre}$ *Sh3bp2*$^{fl/fl}$ mice, the data suggest that loss-of-function of SH3BP2 in osteoclasts is responsible for the reduced bone loss in *Sh3bp2*$^{-/-}$ mice with ligature-induced periodontitis.

SYK deletion in myeloid cells decreases susceptibility to alveolar bone loss in ligature-induced periodontitis

SYK interacts with SH3BP2 and plays an important role in mechanisms for macrophage and osteoclast activation in cherubism mice that harbor a gain-of-function mutation in SH3BP2.[20,33,34] Rescue of inflammatory bone destruction in cherubism mice by selective deletion of SYK in *LysM-Cre* expressing cells suggested that SYK is required for SH3BP2 to regulate osteoclast function in periodontitis.[34] To examine whether SYK in myeloid cells mediates the reduction of susceptibility to alveolar bone loss, *Syk*$^{fl/fl}$ mice were crossed with *LysM-Cre* mice. Homozygous *LysM-Cre* expression was necessary for sufficient *Syk* deletion, which is similar to our finding for *Sh3bp2* deletion (Supplemental Fig. S6). Similar to *Sh3bp2*$^{-/-}$ mice, *LysM*$^{cre/cre}$ *Syk*$^{fl/fl}$ mice showed reduced susceptibility to alveolar bone loss compared to *LysM*$^{cre/cre}$ *Syk*$^{+/+}$ and *LysM*$^{+/+}$ *Sh3bp2*$^{fl/fl}$ mice (Fig. 4A, 4B) without affecting osteoclast induction (Fig. 4C, 4D). mRNA expression levels of genes related to osteoclasts in jawbone and inflammatory cytokines in gingiva were not affected by conditional deletion of *Syk* in *LysM* expressing cells (Supplemental Fig. S7). Conditional deletion of *Syk* in *LysM*-expressing cells in *Sh3bp2*$^{-/-}$ mice further suppressed the alveolar bone loss (Supplemental Fig. S8), indicating that other pathways independent of SH3BP2 is regulating SYK and that SYK controls alveolar bone loss with SH3BP2 in ligature-induced

periodontitis. Collectively, the data suggest that SYK plays an important role in controlling alveolar bone loss by genetically interacting with SH3BP2.

Pharmacological inhibition of SYK with entospletinib reduces bone loss in ligature-induced periodontitis

Because loss-of-function of SH3BP2 reduces alveolar bone resorption without affecting inflammatory response, SH3BP2-mediated signaling pathways may be therapeutic targets to protect against bone loss while maintaining the capability of host immune defense against pathogenic oral microorganisms. However, no chemical inhibitors or neutralizing antibodies are currently available to suppress the adaptor function of SH3BP2. Because SYK is a key signal transducer for SH3BP2, we hypothesized that SYK inhibition may be an alternative approach to suppress SH3BP2-mediated signals. To examine whether pharmacological inhibition of SYK prevents alveolar bone loss, wild-type mice were treated with entospletinib (GS-9973) daily starting from one day before ligature placement (Fig. 5A). We administered 100 mg/kg GS-9973 intraperitoneally, because this dose successfully ameliorated the established inflammation and bone destruction in cherubism mice.[45] We found that bone loss by ligature placement was reduced by 42.1% in males and 41.6% in females in the GS-9973 treatment group (Fig. 5B, 5C). Histomorphometric analysis showed that GS-9973 treatment reduced N.Oc/BS and Oc.S/BS only in males (Fig. 5D, 5E) without affecting ruffled border formation (Fig. 5F) or the percentage of osteoclasts with ruffled borders (data not shown). GS-9973 administration showed no impact on inflammatory cytokine gene levels in gingiva (Supplemental Fig. S9).

In clinical settings, pharmacological treatment of periodontitis will most likely be initiated after onset of the pathological inflammatory cascade in the gingiva. Thus, we next examined whether GS-9973 administration can reduce alveolar bone loss even when administered after ligature placement (Fig. 5G). As significant induction of osteoclasts occurs 2 days after ligature placement (Supplemental Fig. S10A–C), GS-9973 treatment was started 2 days after ligature placement. Mice treated with GS-9973 showed a reduction in alveolar bone loss by 33.4% in males and 23.9% in females (Fig. 5H, 5I). GS-9973 treatment in the experimental group reduced osteoclast induction also only in males (Fig. 5J, 5K) without affecting ruffled border formation (Fig. 5L) or the percentage of osteoclasts with ruffled borders (data not shown). GS-9973 treatment did not affect inflammatory reaction in gingival tissues (Supplemental Fig. S10D). No abnormalities in histology and function of the liver and kidney were observed after GS-9973 administration (Supplemental Fig. S11). These data suggest that SYK inhibitor treatment is effective not only in protection from alveolar bone loss but also in treatment of alveolar bone loss in ligature-induced periodontitis.

Entospletinib suppresses osteoclast differentiation and function *in vitro*

To investigate the mechanism by which GS-9973 reduces bone loss by osteoclasts, GS-9973 was added to *in vitro* osteoclast cultures at the same time as RANKL stimulation. Osteoclasts were induced by RANKL in the presence and absence of TNF-α or IL-1β. GS-9973 treatment suppressed TRAP-positive multinucleated osteoclast formation from BMMs in all conditions in a dose-dependent manner (Fig. 6A). GS-9973 treatment also effectively inhibited the mineral resorption capacity of osteoclasts (Fig. 6B). Since GS-9973

treatment had a protective effect against bone loss when administered 2 days after periodontitis induction (Fig. 5H, 5I), we next investigated whether GS-9973 has an impact on later phases of osteoclastogenesis. GS-9973 was added to BMM cultures 1 or 2 days after RANKL stimulation. We found that osteoclast formation is suppressed even when GS-9973 was added after RANKL stimulation (Fig. 6C). Western blotting showed a reduced induction of NFATc1, MMP9, and Cathepsin K in the presence of GS-9973 (Fig. 6D). SRC protein that is critical for ruffled border formation is induced during osteoclastogenesis.[46–50] Consistent with reduced osteoclast function, SRC protein induction was suppressed in the presence of GS-9973 (Fig. 6D). No osteoclasts with actin ring were formed in the BMM culture stimulated with RANKL in the presence of GS-9973 (Fig. 6E). There was no significant sex difference in the effect of GS-9973 (data not shown). These results confirm that SYK is an important kinase for both osteoclast differentiation and function *in vitro* and that the SYK inhibitor GS-9973 can suppress the SYK signaling pathway at the beginning and in the middle phases of osteoclastogenesis. Taken together, the data suggest that GS-9973 decreases alveolar bone loss in ligature-induced periodontitis by inhibiting the formation of functional osteoclasts.

Discussion

Previously, we have shown that gain-of-function mutations in the adaptor protein SH3BP2 are responsible for cherubism and that mutant SH3BP2 potentiates osteoclast formation and macrophage activation via SYK.[32–34] In contrast, loss-of-function of SH3BP2 has been shown to protect against inflammatory bone loss in mouse models of RA.[39] In this study, we showed that the SH3BP2-SYK pathway, which is the pathogenic pathway responsible for the rare craniofacial disorder cherubism, is also critically involved in the regulation of alveolar bone resorption in a ligature-induced mouse periodontitis model. Therefore, the current study provides a new example for the concept that studying molecular defects in rare craniofacial diseases can result in a better understanding of the basic pathology of more common diseases and lead to opportunities for novel treatment strategies.[51]

In the current clinical practice, standard treatment for periodontal diseases is mechanical debridement of dental plaque harboring pathogenic bacteria to reduce gingival inflammation and subsequent alveolar bone loss. The majority of patients with periodontitis respond favorably to the standard treatment, but some patients diagnosed with aggressive periodontitis, which affects younger populations, do not respond to the treatment and show rapid progression of periodontal tissue destruction.[52] Therefore, systemic antibiotic treatment has been employed when patients do not respond to conventional mechanical debridement or have acute periodontal infections associated with systemic diseases.[53] However, currently there are no established pharmacological approaches available for the treatment of periodontal bone loss except for antibiotic treatment, which can have other side effects. Here, we showed that genetic ablation of the SH3BP2-SYK axis in myeloid lineage cells reduces bone resorption in a ligature-induced experimental periodontitis model. Furthermore, pharmacological inhibition of SYK with GS-9973 exhibited the same protective effect against alveolar bone loss. These findings indicate that SYK inhibition may be a new treatment option for bone resorption in periodontitis. Notably, the advantage of GS-9973 treatment is that it shows suppressive effect in bone loss even when administered

after periodontitis induction, suggesting that the SYK inhibitor may be able to slow down progressive bone loss in human periodontitis. This is different from anti-IL-17A antibody administration in the same periodontitis model.[8] The SYK inhibitor treatment may meet the requirements of clinical practice, because intragingival injection, which would allow to reduce the dose and frequency of SYK inhibitor administration and lessen the risk for potential adverse events, could be considered as a route for administration in humans. Recent investigations demonstrated that T_H17 cells that produce IL-17A and IL-17F are the primary drivers for the pathogenesis of periodontitis in mice and humans.[8,17] These studies provided mechanistic and genetic justification that inhibition of IL-17 family members or suppression of T_H17 cell development may be a plausible therapeutic option for treatment of alveolar bone resorption in periodontitis. Because anti-SYK treatment preferentially inhibits osteoclastic bone resorption without affecting inflammation, anti-IL-17 therapy in combination with SYK inhibitor may provide a synergistic effect in treating alveolar bone loss.

SH3BP2-deficient mice (*Sh3bp2*$^{-/-}$) are reported to exhibit osteoporosis at 12 weeks of age because of a net effect of impaired osteoblastic bone formation and osteoclastic bone-resorption.[38] However, alveolar bone volume was comparable between the SH3BP2-deficient mice and wild-type controls at 10 weeks of age (Fig. 1B). Because SH3BP2 has a profound impact on both osteoblast and osteoclast function, we aimed to determine the cell type(s) responsible for the protection against alveolar bone loss in SH3BP2-deficient mice. We found that *Sh3bp2*$^{fl/fl}$ mice with *LysM-Cre* expression, which lack SH3BP2 in myeloid lineage cells including osteoclast precursor cells exhibit a reduction in bone loss comparable to mice with global SH3BP2 deficiency (Fig. 1B, 3B). Furthermore, *Sh3bp2* deletion in myeloid cells did not change osteoclast induction on the alveolar bone surface (Fig. 3C, 3D) or expression levels of osteoclast markers and inflammatory cytokines (Supplemental Fig. S5). These data suggest that suppressed osteoclast function rather than osteoclast differentiation is responsible for decreased bone loss in SH3BP2-deficient mice in ligature-induced periodontitis. Indeed, SH3BP2-deficient osteoclast progenitors that are stimulated with RANKL are significantly defective in their bone resorption capacity particularly under inflammatory conditions in cell culture, while maintaining the induction of the master osteoclastogenic transcription factor NFATc1.[38,39] They also fail to develop an organized actin cytoskeleton, which is required for sealing zone formation of bone-resorbing osteoclasts.[38,54] In addition, it has been shown that deletion of *Sh3bp2* in osteoclast progenitors by *LysM-Cre* suppressed *in vitro* osteoclast bone resorption capability.[55] These data establish SH3BP2 as a crucial regulator for osteoclast function rather than for differentiation[38] and support our conclusion that lack of SH3BP2 decreases alveolar bone loss by suppressing osteoclast function.

SYK is a cytoplasmic protein tyrosine kinase predominantly expressed in the hematopoietic cell lineage. SYK signaling mediates diverse immune functions particularly in B cells, neutrophils, macrophages, mast cells, and osteoclasts by coupling immune cell receptors to intracellular signaling pathways.[56] Thus, SYK has been a hopeful drug target for immune and inflammatory disorders including RA and cherubism.[45,57–59] In this study, we employed the SYK inhibitor entospletinib (GS-9973), because this second-generation compound has greater selectivity against SYK than tamatinib (R406), which is the active

metabolite of fostamatinib (R788)[60–63] and has a longer half-life in mouse plasma compared to R406.[61,64] While GS-9973 has relatively high selectivity to tyrosine kinase non-receptor 1 (TNK1, Kd: TNK1 86 nM vs. SYK 10.5 nM)[60,62], the most comprehensive clinical experience of SYK inhibitors to date has been obtained with GS-9973.[63,65] Clinical trials for the use of GS-9973 in certain types of leukemia and lymphoma are currently ongoing (https://clinicaltrials.gov). Because we showed that GS-9973 is highly potent in suppressing alveolar bone loss in a mouse model for periodontitis (Fig. 5) and is capable of inhibiting differentiation and function of osteoclasts *in vitro* (Fig. 6), clinical trials of GS-9973 for periodontal diseases may be contemplated.

Similar to SH3BP2-deficient osteoclasts, SYK-deficient osteoclast precursor cells stimulated with RANKL have deficiencies in forming functional osteoclasts.[66] SYK-deficient osteoclasts have a disturbed cytoskeleton, because they fail to spread or form actin rings *in vitro* and are incapable of adhering to the bone surface *in vivo*.[67,68] However, osteoclast numbers in SYK-deficient chimeric mice are indistinguishable from those in irradiated control animals transplanted with wild-type fetal liver cells whether with or without stimulation with PTH.[67] Despite the clear defects in osteoclast function, SYK-deficient osteoclasts express osteoclastic marker genes and exhibit intracellular signaling activation required for efficient osteoclast differentiation at levels comparable to SYK-sufficient osteoclasts.[66,67] These results demonstrate that genetic depletion of SYK impairs primarily osteoclast function but not differentiation *in vitro* and *in vivo.* We have shown that GS-9973 suppresses osteoclast differentiation and function *in vitro*, suggesting that pharmacological inhibition of SYK by GS-9973 protects against alveolar bone loss by inhibiting osteoclast function and differentiation *in vivo*. However, only male mice exhibited decreased osteoclast numbers after GS-9973 administration (Fig. 5E, 5K), suggesting that GS-9973 is able to inhibit osteoclast differentiation in male mice more efficiently than female mice. The mechanism responsible for this sex difference and the precise role of SYK and GS-9973 in osteoclast differentiation *in vitro and in vivo* need to be further investigated. Importantly, GS-9973 suppressed osteoclast formation of progenitor cells that were already stimulated with RANKL *in vitro*. The great suppressive potency of GS-9973 against osteoclast differentiation and function may restore alveolar bone mass in active and progressive periodontitis patients who failed to respond to standard removal of dental plaque biofilms.

We showed that double knockout of SH3BP2 and SYK in *LysM*-expressing cells increases the protective effect of the SH3BP2 deletion (Supplemental Fig. S8). This result provides a confirmation that there are alternative pathways for activating SYK in osteoclasts other than via SH3BP2 and suggests that SH3BP2 regulates osteoclast function by interacting with SYK. Pro-osteoclastogenic factors other than RANKL may also regulate osteoclast function via SYK phosphorylation in the ligature-induced periodontitis model.

In conclusion, our study demonstrated that the SH3BP2-SYK axis, when dysregulated, is not only responsible for cherubism[34], but also plays a key role in regulating osteoclast function responsible for alveolar bone loss in periodontitis. Anti-resorptive drugs that selectively dampen osteoclast function but not the osteoclast number are expected to be more effective in treating pathological bone loss.[69] Because SYK is especially critical for osteoclast function, we propose that SYK can be a therapeutic target to ameliorate and protect against

alveolar bone resorption driven by functionally active osteoclasts in periodontal diseases. Periodontitis patients may benefit from anti-SYK therapy for preventing tooth loss.

Supplementary Material

Refer to Web version on PubMed Central for supplementary material.

Acknowledgments

Research reported in this publication was supported by the National Institute of Dental and Craniofacial Research (R01DE025870 to YU) as well as by the National Institute of Arthritis and Musculoskeletal and Skin Diseases (R21AR070953 to YU). The content is solely the responsibility of the authors and does not necessarily represent the official views of the NIH. MK is a recipient of a fellowship from the Brain Circulation Program to develop new leaders for international dental education course through international collaborative dental research, Japan and of a fund for young researchers from Japanese Society of Periodontology. TY is a recipient of the Japan Society for the Promotion of Science (JSPS) Overseas Research Fellowship. We appreciate Tianli Zhu at Indiana University School of Dentistry for technical assistance for histology. We also thank Dr. Toshihisa Kawai at Nova Southeastern University for instructing us in procedures for the mouse ligature-induced periodontitis model.

References

1. Hajishengallis G Periodontitis: from microbial immune subversion to systemic inflammation. Nat Rev Immunol. 2015;15(1):30–44. [PubMed: 25534621]
2. Han YW, Wang X. Mobile microbiome: oral bacteria in extra-oral infections and inflammation. J Dent Res. 2013;92(6):485–91. [PubMed: 23625375]
3. Eke PI, Dye BA, Wei L, Slade GD, Thornton-Evans GO, Borgnakke WS, et al. Update on Prevalence of Periodontitis in Adults in the United States: NHANES 2009 to 2012. J Periodontol. 2015;86(5):611–22. [PubMed: 25688694]
4. Darveau RP. Periodontitis: a polymicrobial disruption of host homeostasis. Nat Rev Microbiol. 2010;8(7):481–90. [PubMed: 20514045]
5. Jiao Y, Hasegawa M, Inohara N. Emerging roles of immunostimulatory oral bacteria in periodontitis development. Trends Microbiol. 2014;22(3):157–63. [PubMed: 24433922]
6. Eskan MA, Jotwani R, Abe T, Chmelar J, Lim JH, Liang S, et al. The leukocyte integrin antagonist Del-1 inhibits IL-17-mediated inflammatory bone loss. Nat Immunol. 2012;13(5):465–73. [PubMed: 22447028]
7. Dutzan N, Konkel JE, Greenwell-Wild T, Moutsopoulos NM. Characterization of the human immune cell network at the gingival barrier. Mucosal Immunol. 2016;9(5):1163–72. [PubMed: 26732676]
8. Dutzan N, Kajikawa T, Abusleme L, Greenwell-Wild T, Zuazo CE, Ikeuchi T, et al. A dysbiotic microbiome triggers TH17 cells to mediate oral mucosal immunopathology in mice and humans. Science Translational Medicine. 2018;10(463).
9. Sato K, Suematsu A, Okamoto K, Yamaguchi A, Morishita Y, Kadono Y, et al. Th17 functions as an osteoclastogenic helper T cell subset that links T cell activation and bone destruction. J Exp Med. 2006;203(12):2673–82. [PubMed: 17088434]
10. Komatsu N, Okamoto K, Sawa S, Nakashima T, Oh-hora M, Kodama T, et al. Pathogenic conversion of Foxp3+ T cells into TH17 cells in autoimmune arthritis. Nat Med. 2014;20(1):62–8. [PubMed: 24362934]
11. Weinreb M, Quartuccio H, Seedor JG, Aufdemorte TB, Brunsvold M, Chaves E, et al. Histomorphometrical analysis of the effects of the bisphosphonate alendronate on bone loss caused by experimental periodontitis in monkeys. J Periodontal Res. 1994;29(1):35–40. [PubMed: 8113951]
12. Sveen K, Skaug N. Bone resorption stimulated by lipopolysaccharides from Bacteroides, Fusobacterium and Veillonella, and by the lipid A and the polysaccharide part of Fusobacterium lipopolysaccharide. Scand J Dent Res. 1980;88(6):535–42. [PubMed: 7017892]

13. Jiao Y, Hasegawa M, Inohara N. The Role of Oral Pathobionts in Dysbiosis during Periodontitis Development. J Dent Res. 2014;93(6):539–46. [PubMed: 24646638]
14. Kong YY, Yoshida H, Sarosi I, Tan HL, Timms E, Capparelli C, et al. OPGL is a key regulator of osteoclastogenesis, lymphocyte development and lymph-node organogenesis. Nature. 1999;397(6717):315–23. [PubMed: 9950424]
15. Lacey DL, Timms E, Tan HL, Kelley MJ, Dunstan CR, Burgess T, et al. Osteoprotegerin ligand is a cytokine that regulates osteoclast differentiation and activation. Cell. 1998;93(2):165–76. [PubMed: 9568710]
16. Kim N, Odgren PR, Kim DK, Marks SC Jr., Choi Y Diverse roles of the tumor necrosis factor family member TRANCE in skeletal physiology revealed by TRANCE deficiency and partial rescue by a lymphocyte-expressed TRANCE transgene. Proc Natl Acad Sci U S A. 2000;97(20): 10905–10. [PubMed: 10984520]
17. Tsukasaki M, Komatsu N, Nagashima K, Nitta T, Pluemsakunthai W, Shukunami C, et al. Host defense against oral microbiota by bone-damaging T cells. Nat Commun. 2018;9(1):701. [PubMed: 29453398]
18. Graves DT, Alshabab A, Albiero ML, Mattos M, Correa JD, Chen S, et al. Osteocytes play an important role in experimental periodontitis in healthy and diabetic mice through expression of RANKL. J Clin Periodontol. 2018;45(3):285–92. [PubMed: 29220094]
19. Li JY, Yu M, Tyagi AM, Vaccaro C, Hsu E, Adams J, et al. IL-17 Receptor Signaling in Osteoblasts/Osteocytes Mediates PTH-Induced Bone Loss and Enhances Osteocytic RANKL Production. J Bone Miner Res. 2019;34(2):349–60. [PubMed: 30399207]
20. Deckert M, Tartare-Deckert S, Hernandez J, Rottapel R, Altman A. Adaptor function for the Syk kinases-interacting protein 3BP2 in IL-2 gene activation. Immunity. 1998;9(5):595–605. [PubMed: 9846481]
21. Jevremovic D, Billadeau DD, Schoon RA, Dick CJ, Leibson PJ. Regulation of NK cell-mediated cytotoxicity by the adaptor protein 3BP2. J Immunol. 2001;166(12):7219–28. [PubMed: 11390470]
22. Foucault I, Liu YC, Bernard A, Deckert M. The chaperone protein 14–3-3 interacts with 3BP2/SH3BP2 and regulates its adapter function. J Biol Chem. 2003;278(9):7146–53. [PubMed: 12501243]
23. Maeno K, Sada K, Kyo S, Miah SM, Kawauchi-Kamata K, Qu X, et al. Adaptor protein 3BP2 is a potential ligand of Src homology 2 and 3 domains of Lyn protein-tyrosine kinase. J Biol Chem. 2003;278(27):24912–20. [PubMed: 12709437]
24. Foucault I, Le Bras S, Charvet C, Moon C, Altman A, Deckert M. The adaptor protein 3BP2 associates with VAV guanine nucleotide exchange factors to regulate NFAT activation by the B-cell antigen receptor. Blood. 2005;105(3):1106–13. [PubMed: 15345594]
25. Shukla U, Hatani T, Nakashima K, Ogi K, Sada K. Tyrosine phosphorylation of 3BP2 regulates B cell receptor-mediated activation of NFAT. J Biol Chem. 2009;284(49):33719–28. [PubMed: 19833725]
26. Chihara K, Nakashima K, Takeuchi K, Sada K. Association of 3BP2 with SHP-1 regulates SHP-1-mediated production of TNF-α in RBL-2H3 cells. Genes to Cells. 2011;16(12):1133–45. [PubMed: 22077594]
27. Chen G, Dimitriou I, Milne L, Lang KS, Lang PA, Fine N, et al. The 3BP2 adapter protein is required for chemoattractant-mediated neutrophil activation. J Immunol. 2012;189(5):2138–50. [PubMed: 22815290]
28. Ainsua-Enrich E, Alvarez-Errico D, Gilfillan AM, Picado C, Sayos J, Rivera J, et al. The adaptor 3BP2 is required for early and late events in FcepsilonRI signaling in human mast cells. J Immunol. 2012;189(6):2727–34. [PubMed: 22896635]
29. Ainsua-Enrich E, Serrano-Candelas E, Alvarez-Errico D, Picado C, Sayos J, Rivera J, et al. The adaptor 3BP2 is required for KIT receptor expression and human mast cell survival. J Immunol. 2015;194(9):4309–18. [PubMed: 25810396]
30. Chihara K, Kato Y, Yoshiki H, Takeuchi K, Fujieda S, Sada K. Syk-dependent tyrosine phosphorylation of 3BP2 is required for optimal FcRgamma-mediated phagocytosis and chemokine expression in U937 cells. Sci Rep. 2017;7(1):11480. [PubMed: 28904407]

31. Dimitriou ID, Lee K, Akpan I, Lind EF, Barr VA, Ohashi PS, et al. Timed Regulation of 3BP2 Induction Is Critical for Sustaining CD8(+) T Cell Expansion and Differentiation. Cell Rep. 2018;24(5):1123–35. [PubMed: 30067970]
32. Ueki Y, Tiziani V, Santanna C, Fukai N, Maulik C, Garfinkle J, et al. Mutations in the gene encoding c-Abl-binding protein SH3BP2 cause cherubism. Nat Genet. 2001;28(2):125–6. [PubMed: 11381256]
33. Ueki Y, Lin CY, Senoo M, Ebihara T, Agata N, Onji M, et al. Increased myeloid cell responses to M-CSF and RANKL cause bone loss and inflammation in SH3BP2 “cherubism” mice. Cell. 2007;128(1):71–83. [PubMed: 17218256]
34. Yoshitaka T, Mukai T, Kittaka M, Alford LM, Masrani S, Ishida S, et al. Enhanced TLR-MYD88 signaling stimulates autoinflammation in SH3BP2 cherubism mice and defines the etiology of cherubism. Cell Rep. 2014;8(6):1752–66. [PubMed: 25220465]
35. Mukai T, Ishida S, Ishikawa R, Yoshitaka T, Kittaka M, Gallant R, et al. SH3BP2 cherubism mutation potentiates TNF-alpha-induced osteoclastogenesis via NFATc1 and TNF-alpha-mediated inflammatory bone loss. J Bone Miner Res. 2014;29(12):2618–35. [PubMed: 24916406]
36. Mukai T, Gallant R, Ishida S, Yoshitaka T, Kittaka M, Nishida K, et al. SH3BP2 gain-of-function mutation exacerbates inflammation and bone loss in a murine collagen-induced arthritis model. PLoS One. 2014;9(8):e105518. [PubMed: 25144740]
37. Nagasu A, Mukai T, Iseki M, Kawahara K, Tsuji S, Nagasu H, et al. Sh3bp2 Gain-Of-Function Mutation Ameliorates Lupus Phenotypes in B6.MRL-Fas(lpr) Mice. Cells. 2019;8(5).
38. Levaot N, Simoncic PD, Dimitriou ID, Scotter A, La Rose J, Ng AH, et al. 3BP2-deficient mice are osteoporotic with impaired osteoblast and osteoclast functions. J Clin Invest. 2011;121(8):3244–57. [PubMed: 21765218]
39. Mukai T, Gallant R, Ishida S, Kittaka M, Yoshitaka T, Fox DA, et al. Loss of SH3 domain-binding protein 2 function suppresses bone destruction in tumor necrosis factor-driven and collagen-induced arthritis in mice. Arthritis Rheumatol. 2015;67(3):656–67. [PubMed: 25470448]
40. Chen G, Dimitriou ID, La Rose J, Ilangumaran S, Yeh WC, Doody G, et al. The 3BP2 adapter protein is required for optimal B-cell activation and thymus-independent type 2 humoral response. Mol Cell Biol. 2007;27(8):3109–22. [PubMed: 17283041]
41. Wang Q, Garrity GM, Tiedje JM, Cole JR. Naive Bayesian classifier for rapid assignment of rRNA sequences into the new bacterial taxonomy. Appl Environ Microbiol. 2007;73(16):5261–7. [PubMed: 17586664]
42. Abe T, Hajishengallis G. Optimization of the ligature-induced periodontitis model in mice. J Immunol Methods. 2013;394(1-2):49–54. [PubMed: 23672778]
43. Jiao Y, Darzi Y, Tawaratsumida K, Marchesan JT, Hasegawa M, Moon H, et al. Induction of bone loss by pathobiont-mediated Nod1 signaling in the oral cavity. Cell Host Microbe. 2013;13(5):595–601. [PubMed: 23684310]
44. de la Fuente MA, Kumar L, Lu B, Geha RS. 3BP2 deficiency impairs the response of B cells, but not T cells, to antigen receptor ligation. Mol Cell Biol. 2006;26(14):5214–25. [PubMed: 16809760]
45. Yoshimoto T, Hayashi T, Kondo T, Kittaka M, Reichenberger EJ, Ueki Y. Second-Generation SYK Inhibitor Entospletinib Ameliorates Fully Established Inflammation and Bone Destruction in the Cherubism Mouse Model. J Bone Miner Res. 2018;33(8):1513–19. [PubMed: 29669173]
46. Soriano P, Montgomery C, Geske R, Bradley A. Targeted disruption of the c-src proto-oncogene leads to osteopetrosis in mice. Cell. 1991;64(4):693–702. [PubMed: 1997203]
47. Horne WC, Neff L, Chatterjee D, Lomri A, Levy JB, Baron R. Osteoclasts express high levels of pp60c-src in association with intracellular membranes. J Cell Biol. 1992;119(4):1003–13. [PubMed: 1385441]
48. Boyce BF, Yoneda T, Lowe C, Soriano P, Mundy GR. Requirement of pp60c-src expression for osteoclasts to form ruffled borders and resorb bone in mice. J Clin Invest. 1992;90(4):1622–7. [PubMed: 1383278]
49. Abu-Amer Y, Ross FP, Edwards J, Teitelbaum SL. Lipopolysaccharide-stimulated osteoclastogenesis is mediated by tumor necrosis factor via its P55 receptor. J Clin Invest. 1997;100(6):1557–65. [PubMed: 9294124]

50. Zhang YH, Heulsmann A, Tondravi MM, Mukherjee A, Abu-Amer Y. Tumor necrosis factor-alpha (TNF) stimulates RANKL-induced osteoclastogenesis via coupling of TNF type 1 receptor and RANK signaling pathways. J Biol Chem. 2001;276(1):563–8. [PubMed: 11032840]
51. Boycott KM, Vanstone MR, Bulman DE, MacKenzie AE. Rare-disease genetics in the era of next-generation sequencing: discovery to translation. Nat Rev Genet. 2013;14(10):681–91. [PubMed: 23999272]
52. Page RC, Altman LC, Ebersole JL, Vandesteen GE, Dahlberg WH, Williams BL, et al. Rapidly progressive periodontitis. A distinct clinical condition. J Periodontol. 1983;54(4):197–209. [PubMed: 6574228]
53. Slots J Systemic antibiotics in periodontics. J Periodontol. 2004;75(11):1553–65.
54. Prod'Homme V, Boyer L, Dubois N, Mallavialle A, Munro P, Mouska X, et al. Cherubism allele heterozygosity amplifies microbe-induced inflammatory responses in murine macrophages. J Clin Invest. 2015;125(4):1396–400. [PubMed: 25705883]
55. Matsumoto Y, Larose J, Kent OA, Lim M, Changoor A, Zhang L, et al. RANKL coordinates multiple osteoclastogenic pathways by regulating expression of ubiquitin ligase RNF146. J Clin Invest. 2017;127(4):1303–15. [PubMed: 28287403]
56. Mocsai A, Ruland J, Tybulewicz VL. The SYK tyrosine kinase: a crucial player in diverse biological functions. Nat Rev Immunol. 2010;10(6):387–402. [PubMed: 20467426]
57. Geahlen RL. Getting Syk: spleen tyrosine kinase as a therapeutic target. Trends Pharmacol Sci. 2014;35(8):414–22. [PubMed: 24975478]
58. Braselmann S, Taylor V, Zhao H, Wang S, Sylvain C, Baluom M, et al. R406, an orally available spleen tyrosine kinase inhibitor blocks fc receptor signaling and reduces immune complex-mediated inflammation. J Pharmacol Exp Ther. 2006;319(3):998–1008. [PubMed: 16946104]
59. Pine PR, Chang B, Schoettler N, Banquerigo ML, Wang S, Lau A, et al. Inflammation and bone erosion are suppressed in models of rheumatoid arthritis following treatment with a novel Syk inhibitor. Clin Immunol. 2007;124(3):244–57. [PubMed: 17537677]
60. Burke RT, Meadows S, Loriaux MM, Currie KS, Mitchell SA, Maciejewski P, et al. A potential therapeutic strategy for chronic lymphocytic leukemia by combining Idelalisib and GS-9973, a novel spleen tyrosine kinase (Syk) inhibitor. Oncotarget. 2014;5(4):908–15. [PubMed: 24659719]
61. Currie KS, Kropf JE, Lee T, Blomgren P, Xu J, Zhao Z, et al. Discovery of GS-9973, a selective and orally efficacious inhibitor of spleen tyrosine kinase. J Med Chem. 2014;57(9):3856–73. [PubMed: 24779514]
62. Sharman J, Hawkins M, Kolibaba K, Boxer M, Klein L, Wu M, et al. An open-label phase 2 trial of entospletinib (GS-9973), a selective spleen tyrosine kinase inhibitor, in chronic lymphocytic leukemia. Blood. 2015;125(15):2336–43. [PubMed: 25696919]
63. Liu D, Mamorska-Dyga A. Syk inhibitors in clinical development for hematological malignancies. J Hematol Oncol. 2017;10(1):145. [PubMed: 28754125]
64. Suljagic M, Longo PG, Bennardo S, Perlas E, Leone G, Laurenti L, et al. The Syk inhibitor fostamatinib disodium (R788) inhibits tumor growth in the Emu-TCL1 transgenic mouse model of CLL by blocking antigen-dependent B-cell receptor signaling. Blood. 2010;116(23):4894–905. [PubMed: 20716772]
65. Sharman J, Di Paolo J. Targeting B-cell receptor signaling kinases in chronic lymphocytic leukemia: the promise of entospletinib. Ther Adv Hematol. 2016;7(3):157–70. [PubMed: 27247756]
66. Mocsai A, Humphrey MB, Van Ziffle JA, Hu Y, Burghardt A, Spusta SC, et al. The immunomodulatory adapter proteins DAP12 and Fc receptor gamma-chain (FcRgamma) regulate development of functional osteoclasts through the Syk tyrosine kinase. Proc Natl Acad Sci U S A. 2004;101(16):6158–63. [PubMed: 15073337]
67. Zou W, Kitaura H, Reeve J, Long F, Tybulewicz VL, Shattil SJ, et al. Syk, c-Src, the alphavbeta3 integrin, and ITAM immunoreceptors, in concert, regulate osteoclastic bone resorption. J Cell Biol. 2007;176(6):877–88. [PubMed: 17353363]
68. Faccio R, Zou W, Colaianni G, Teitelbaum SL, Ross FP. High dose M-CSF partially rescues the Dap12−/− osteoclast phenotype. J Cell Biochem. 2003;90(5):871–83. [PubMed: 14624447]

69. Teitelbaum SL. Therapeutic implications of suppressing osteoclast formation versus function. Rheumatology (Oxford). 2016;55(suppl 2):ii61–ii63. [PubMed: 27856662]

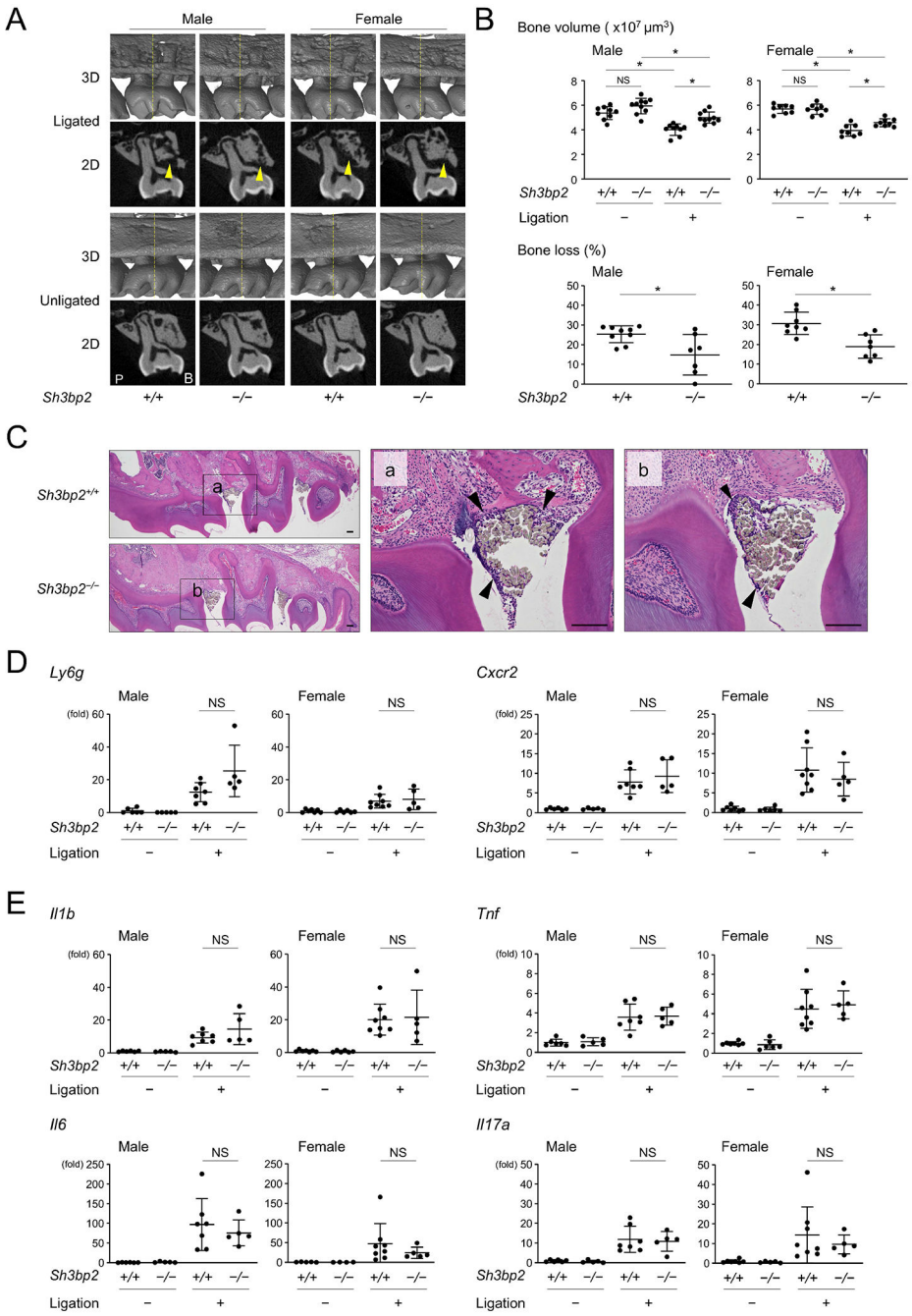

Figure 1. Loss-of-function of SH3BP2 reduces alveolar bone loss in ligature-induced periodontitis.

(A) Two-dimensional (2D) coronal plane μCT images through the middle of maxillary second molar (bottom) and three-dimensional (3D) μCT images surrounding the maxillary second molar (top). Yellow arrowheads indicate areas of alveolar bone loss. Yellow line in 3D image indicates the coronal plane for 2D image. P: palatal side. B: buccal side. (B) Alveolar bone volume and percentage (%) of bone loss against contralateral unligated side. (C) H&E staining of sagittal plane sections of maxilla. Arrowheads indicate inflammatory infiltrates underneath the ligated silk sutures. 10-week-old male mice. Bar = 100 μm. (D, E)

qPCR analysis with RNA isolated from gingiva. Average levels in unligated wild-type mice were set as 1. Data are presented as mean ± SD. *$p < 0.05$. NS = not significant. Student's t-test for bone loss in (B) or ANOVA with Tukey-Kramer post hoc test for bone volume in (B) and in (D, E).

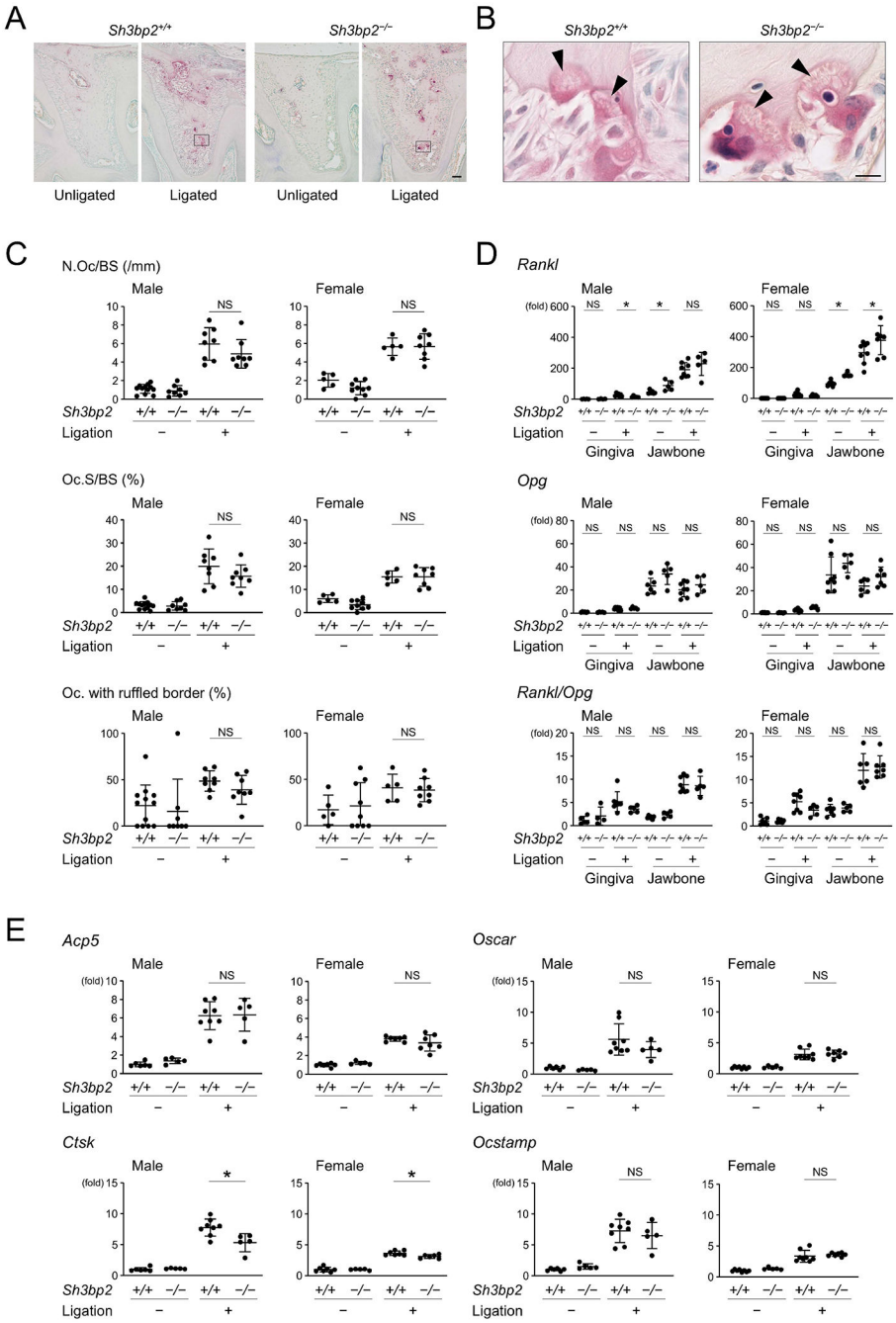

Figure 2. Loss-of-function of SH3BP2 does not affect induction of osteoclast formation in ligature-induced periodontitis.

(A, B) TRAP staining of alveolar bone between two buccal roots of the ligated second molar. Arrowheads indicate ruffled borders. Images in (B) are high magnification of the boxed area in (A). 10-week-old male mice. Bar = 100 and 10 μm, respectively. (C) Histomorphometric analysis for TRAP-positive cells. (D) qPCR analysis for *Rankl* and *Opg* expression and their ratio in gingiva and alveolar bone. Average levels in gingiva of unligated wild-type mice were set as 1. (E) qPCR analysis for osteoclast marker genes using RNA from alveolar bone. Average levels in unligated wild-type mice were set as 1. Data are

presented as mean ± SD. *$p < 0.05$. NS = not significant. Student's *t*-test (D) or ANOVA with Tukey-Kramer post hoc test (C, E).

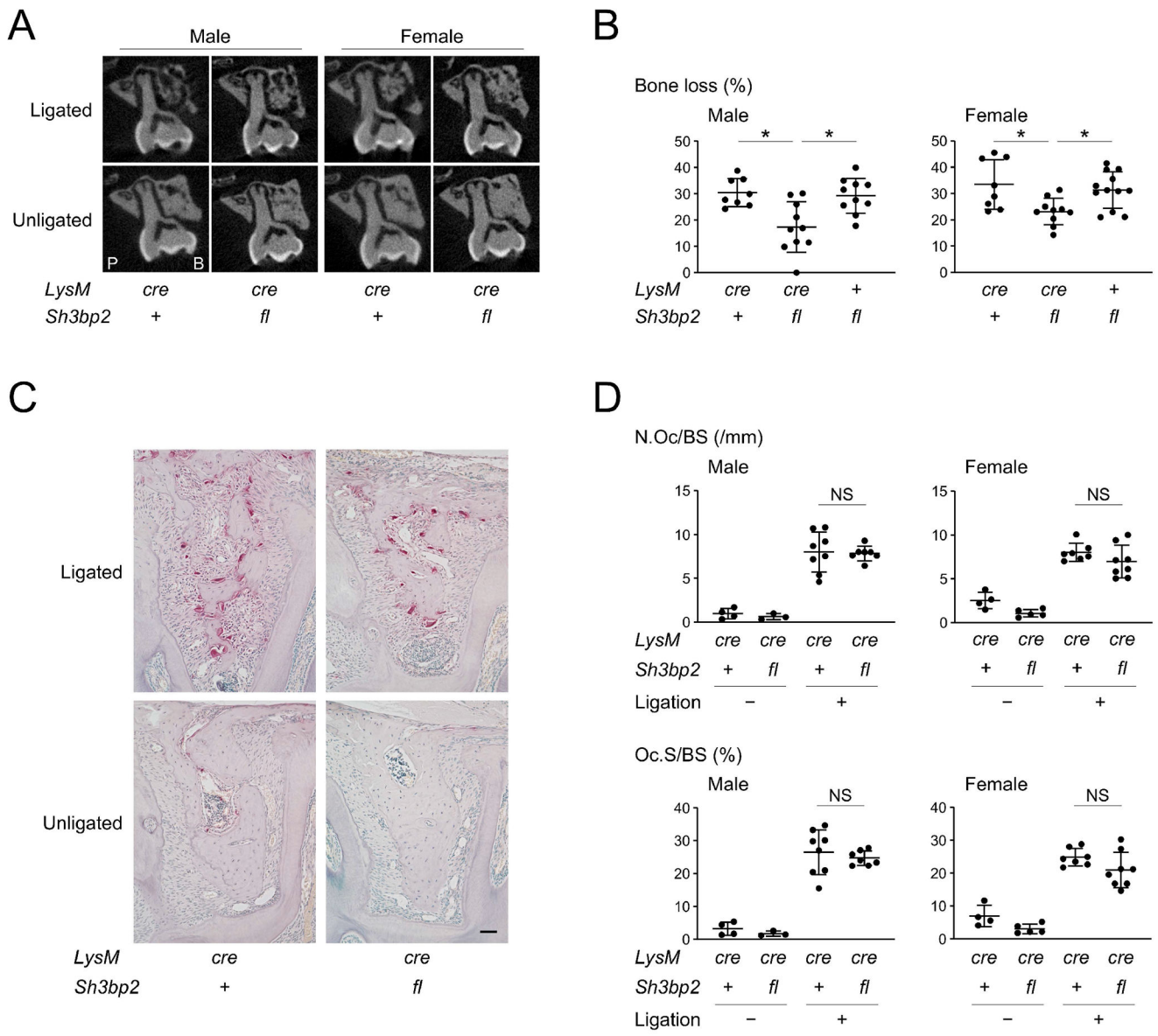

Figure 3. SH3BP2 in myeloid cells regulates susceptibility to alveolar bone loss in ligature-induced periodontitis.

(A) Two-dimensional coronal plane μCT images through the middle of maxillary second molar. P: palatal side. B: buccal side. (B) Percentage (%) of alveolar bone loss against contralateral unligated side. (C) TRAP staining of alveolar bone between two buccal roots of the ligated second molar. 10-week-old male mice. Bar = 100 μm. (D) Histomorphometric analysis for TRAP-positive cells. Data are presented as mean ± SD. *$p < 0.05$. NS = not significant. ANOVA with Tukey-Kramer post hoc test. + = +/+, *cre* = *cre/cre*, *fl* = *fl/fl*.

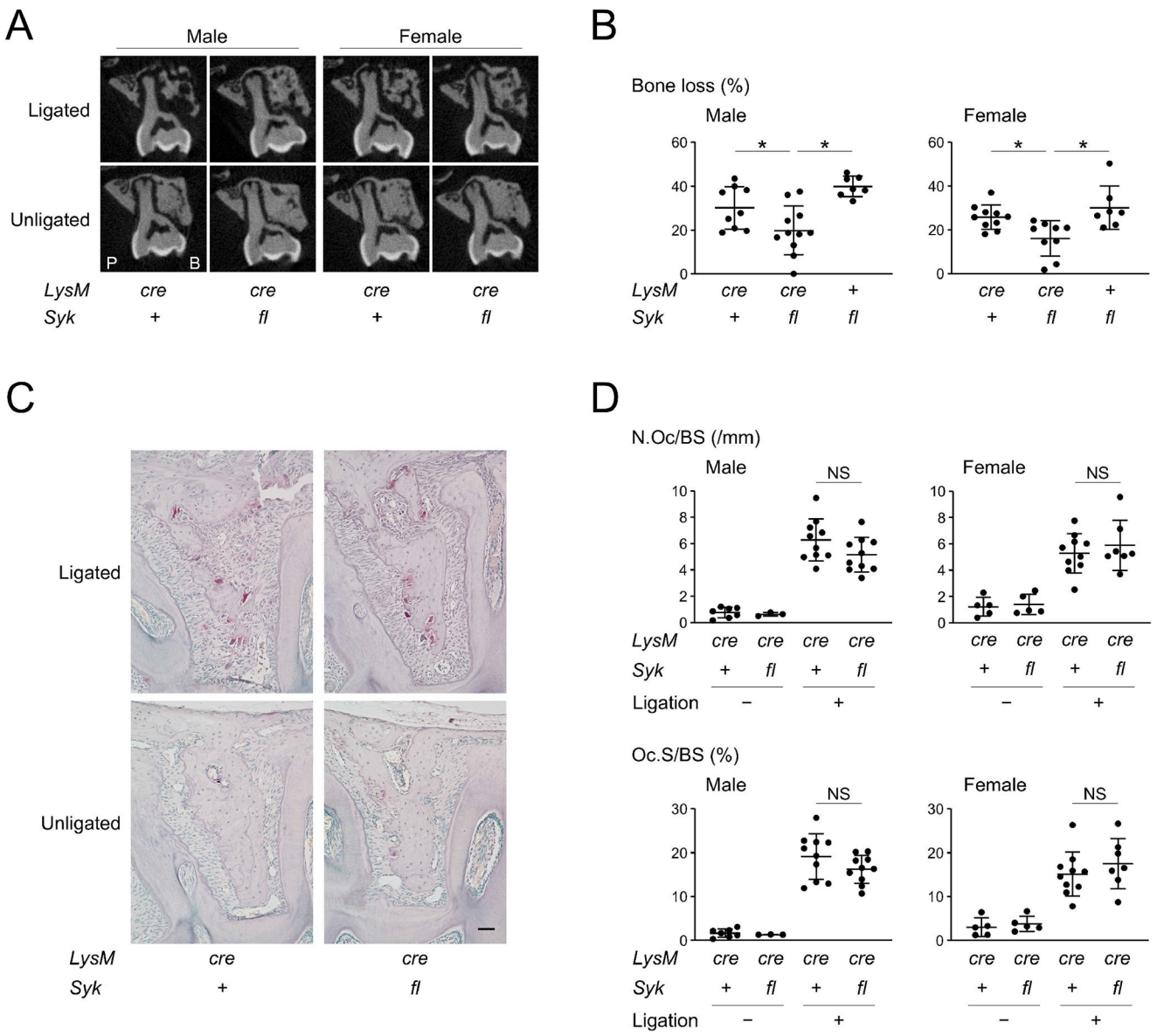

Figure 4. SYK deletion in myeloid cells decreases susceptibility to bone loss in ligature-induced periodontitis.

(A) Two-dimensional coronal plane μCT images through the middle of maxillary second molar. P: palatal side. B: buccal side. (B) Percentage (%) of alveolar bone loss against contralateral unligated side. (C) TRAP staining of alveolar bone between two buccal roots of the ligated second molar. 10-week-old male mice. Bar = 100 μm. (D) Histomorphometric analysis for TRAP-positive cells. Data are presented as mean ± SD. *$p < 0.05$. NS = not significant. ANOVA with Tukey-Kramer post hoc test. + = +/+, *cre* = *cre/cre, fl* = *fl/fl*.

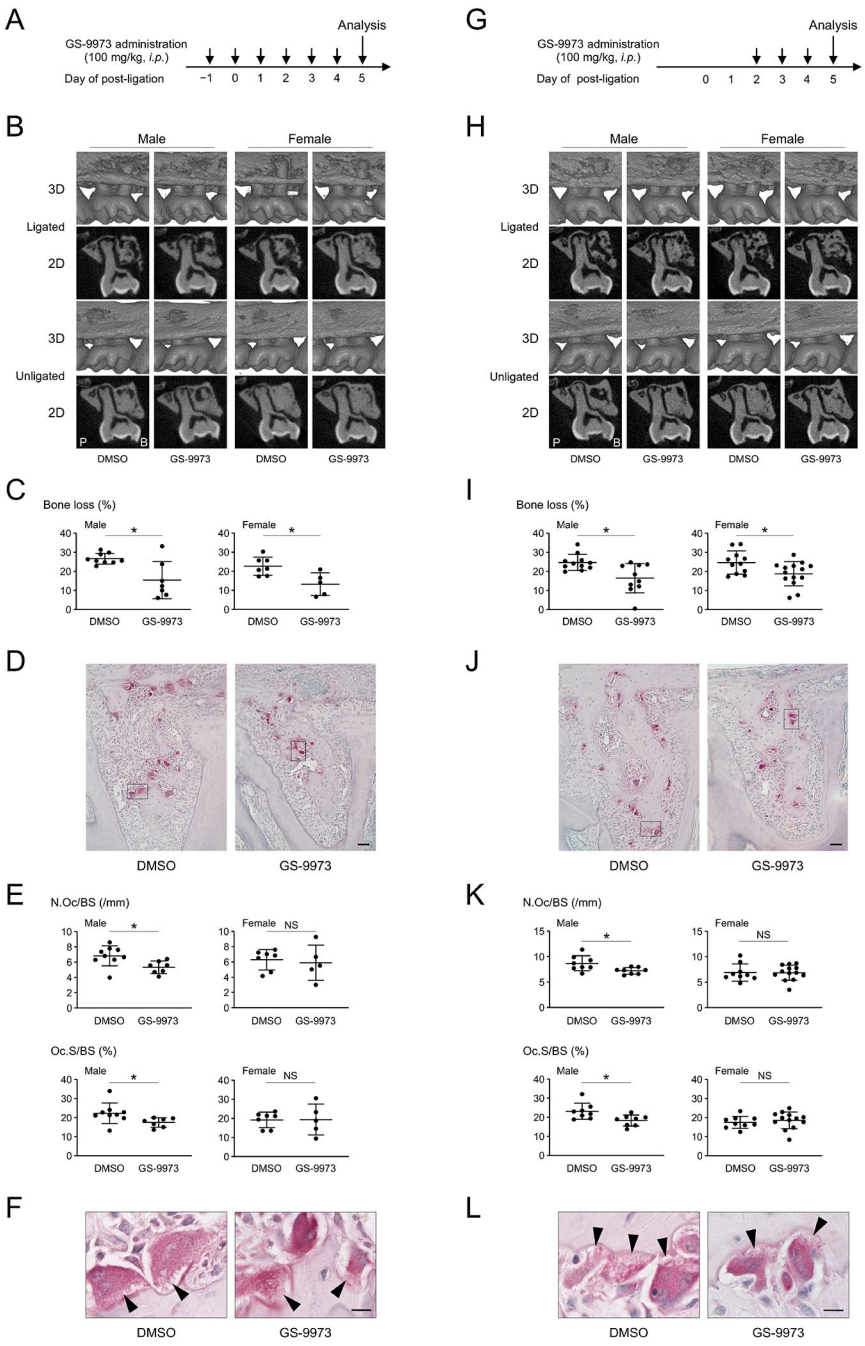

Figure 5. SYK inhibitor GS-9973 restores alveolar bone volume in ligature-induced periodontitis.

(A) Procedure of GS-9973 administration started one day before ligature placement. (B) Two-dimensional (2D) coronal plane μCT images through the middle of maxillary second molar (bottom) and three-dimensional (3D) μCT images surrounding the maxillary second molar (top). P: palatal side. B: buccal side. (C) Percentage (%) of alveolar bone loss against contralateral unligated side. (D) TRAP staining of alveolar bone between two buccal roots of the ligated second molar. 10-week-old male mice. Bar = 100 μm. (E) Histomorphometric analysis for TRAP-positive cells. $p = 0.0195$ (male) & 0.7118 (female) for N.Oc/BS. $p =$

0.0472 (male) & 0.9751 (female) for Oc.S/BS. (F) TRAP-positive osteoclasts with ruffled borders indicated by arrowheads. High magnification of the boxed area in (D). 10-week-old male mice. Bar = 10 μm. (G) Procedure of GS-9973 administration started two days after ligature placement. (H) 2D coronal plane μCT images through the middle of maxillary second molar (bottom) and 3D μCT images surrounding the maxillary second molar (top). P: palatal side. B: buccal side. (I) Percentage (%) of alveolar bone loss against contralateral unligated side. (J) TRAP staining of alveolar bone between two buccal roots of the ligated second molar. 10-week-old male mice. Bar = 100 μm. (K) Histomorphometric analysis for TRAP-positive cells. $p = 0.0216$ (male) & 0.9469 (female) for N.Oc/BS. $p = 0.0185$ (male) & 0.5551 (female) for Oc.S/BS. (L) TRAP-positive osteoclasts with ruffled borders indicated by arrowheads. High magnification of the boxed area in (J). 10-week-old male mice. Bar = 10 μm. Data are presented as mean ± SD. *$p < 0.05$. NS = not significant. Student's *t*-test.

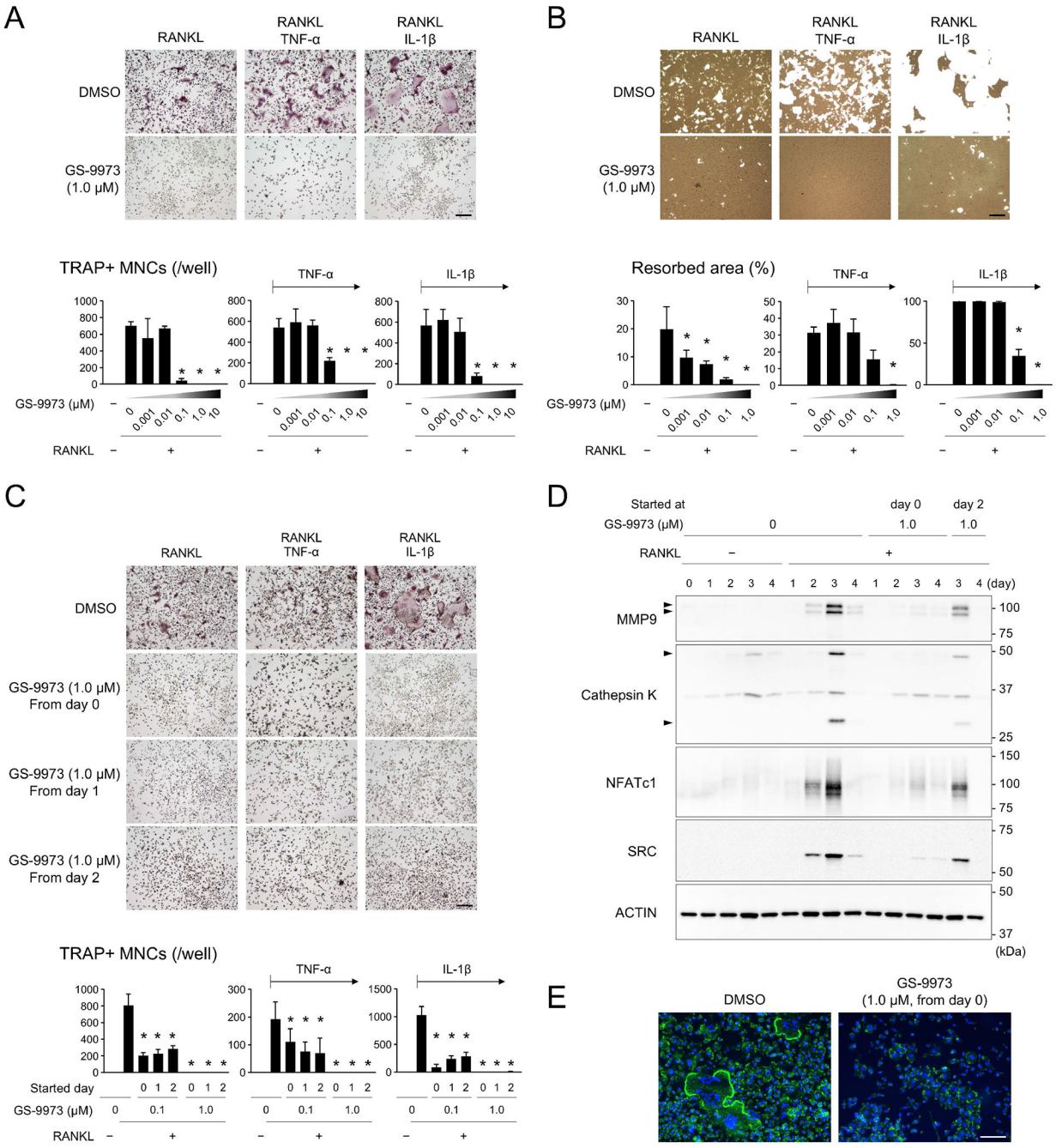

Figure 6. SYK inhibitor GS-9973 suppresses osteoclast differentiation and function *in vitro*.

(A) TRAP-positive osteoclast formation in the presence of GS-9973. BMMs were stimulated with RANKL (50 ng/mL), or RANKL/TNF-α (100 ng/mL), or RANKL/IL-1β (10 ng/mL) in the absence or presence of GS-9973 for 3 days. (B) Resorption assay for calcium phosphate. BMMs stimulated with RANKL, RANKL/TNF-α, or RANKL/IL-1β were cultured with or without GS-9973 for 10 days. Cells were removed and remaining calcium phosphate was stained with silver nitrate to visualize resorbed area. (C) TRAP-positive osteoclast formation in the presence of GS-9973. BMMs were stimulated with RANKL, or

RANKL/TNF-α, or RANKL/IL-1β for 3 days. GS-9973 treatment was started at the same time as RANKL stimulation or 1 or 2 days after RANKL stimulation (day 0, day 1, and day 2, respectively). (D) Western blot analysis of osteoclast-associated proteins. BMMs were stimulated with RANKL for up to 4 days in the absence or presence of GS-9973. (E) Actin ring staining with phalloidin conjugated with Alexa Fluor488. BMMs were stimulated with RANKL for 3 days. (A-E) Culture studies with male wild-type BMMs. (A, B, C, E) Bar = 100 μm. Data are presented as mean ± SD. *$p < 0.05$ with ANOVA with Tukey-Kramer post hoc test.